

ORIGINAL ARTICLE

Loss of gastric interstitial cells of Cajal in patients with hereditary transthyretin amyloidosis

Jonas Wixner¹, Konen Obayashi², Yukio Ando², Pontus Karling¹, and Intissar Anan¹

¹Department of Public Health and Clinical Medicine, Umeå University, Umeå, Sweden and ²Department of Diagnostic Medicine, Graduate School of Medical Sciences, Kumamoto University, Kumamoto, Japan

Abstract

Background: Hereditary transthyretin (TTR) amyloidosis is a systemic neuropathic disorder caused by TTR gene mutations. Gastrointestinal complications are common and the underlying mechanisms remain unclear. The interstitial cells of Cajal (ICC) function as pacemaker cells in the gastrointestinal tract and are important for gastrointestinal motility. The aim of this study was to investigate the densities of gastric ICC and nerves in patients with TTR amyloidosis compared to non-amyloidosis controls.

Methods: Antral wall autopsy specimens from 11 Japanese ATTR V30M patients and 10 controls were analyzed with immunohistochemistry and computerized analysis. Antibodies to c-Kit and TMEM16A were used to assess ICC and an antibody to PGP 9.5 was used to assess nervous tissue. The study was approved by a Japanese ethical committee.

Results: The densities of c-Kit-immunoreactive (IR) ICC were significantly lower in the circular and longitudinal muscle layers of patients compared to controls ($p = 0.004$ for both). Equivalent results were found for TMEM16A-IR ICC. There were no significant differences in PGP 9.5-IR cells in the circular or longitudinal muscle layers between patients and controls ($p = 0.173$ and 0.099 , respectively).

Conclusions: A loss of gastrointestinal ICC may be an important factor for the digestive disturbances in hereditary TTR amyloidosis.

Abbreviations: AGE, advanced glycation end-products; AMI, acute myocardial infarction; ATTR, amyloidogenic transthyretin; FAP, familial amyloid polyneuropathy; GI, gastrointestinal; ICC, interstitial cells of Cajal; IGF-1, insulin-like growth factor 1; IR, immunoreactive; mBMI, modified body mass index; PGP, protein gene product; RAGE, receptor for advanced glycation end-products; TTR, transthyretin; V30M, methionine substituted for valine at position 30

Introduction

Hereditary transthyretin amyloidosis or familial amyloid polyneuropathy (FAP) is a dominantly inherited amyloidosis that is caused by mutated transthyretin (TTR). There are over 100 known amyloidogenic transthyretin (ATTR) missense mutations of which the TTR V30M (methionine substituted for valine at position 30) mutation is the most common [1]. The ATTR mutations cause a decreased stability of the TTR tetramer making it more prone to separate into misfolded monomers, which, in turn, assemble into the beta-pleated sheets that build up the amyloid fibrils [2]. The pathogenesis of TTR amyloidosis is not fully elucidated, but amyloid toxicity seems to play a key role [3,4].

Hereditary TTR amyloidosis is a rare disease, but is present all over the world with endemic areas in Portugal,

Brazil, Sweden and Japan. Symptoms are caused by the deposition of amyloid fibrils in various body tissues and include, for example, peripheral polyneuropathy, autonomic neuropathy, cardiomyopathy, impaired vision, carpal tunnel syndrome and gastrointestinal (GI) disturbances. Without treatment the average survival of Swedish ATTR V30M patients is 9–13 years after onset [5,6] and death is caused by severe malnutrition and opportunistic infections in many cases [6,7]. The most effective treatment, to this date, is a liver transplantation that halts the formation of TTR amyloid from mutated TTR.

The GI complications develop in virtually all patients during the course of the disease [7,8]. Constipation is commonly encountered, and is later relieved by bursts of diarrhoea that successively become permanent. Nausea and vomiting are also reported by many patients. The GI disturbances often lead to malnutrition, which negatively affects the outcome of liver transplantation [9], and are hence important for disease mortality.

The mechanisms behind the GI symptoms in TTR amyloidosis are not clear, but previous studies have shown

an autonomic dysfunction caused by amyloid deposits in the autonomic nervous systems and changes in the enteric nervous system and the neuroendocrine system of the GI tract [10–14].

The interstitial cells of Cajal (ICC) are mesenchymal cells that generate electrical pacemaker activity and mediate nerve-smooth muscle interactions in the GI tract and are therefore important for GI motility. ICC are rich in mitochondria and endoplasmic reticulum but have few contractile elements. A decrease in the number of ICC is believed to be one of the mechanisms behind the GI dysmotilities in, for example, diabetes mellitus [15]. The aim of this study was to investigate the densities of gastric ICC and gastric nerves in patients with hereditary TTR amyloidosis compared to non-amyloidosis controls.

Methods

Patients

Eleven deceased Japanese ATTR V30M patients were included (six women and five men) and all had died from complications of their TTR amyloidosis. The control group consisted of ten deceased Japanese individuals without amyloidosis (seven men and three women), for which five had died of colon cancer, two of acute myocardial infarction, one of lymphoma, one of lung cancer and one of adult T-cell leukaemia. Full-thickness gastric antrum wall samples were collected during autopsies both in patients and controls. The vast majority of the autopsies were performed within 1–5 h post mortem by a pathologist on call. For one patient the autopsy was performed 12 hours post mortem. All post-mortem samples were formalin fixed, paraffin embedded and cross-sectionally cut into 10 µm thick sections.

Nutritional status

The modified body mass index (mBMI), in which the BMI (kg/m^2) was multiplied with serum albumin (g/L) to compensate for oedema [6], was used to assess the nutritional status. Values below 750 were considered consistent with underweight and values below 600 were regarded as consistent with severe malnutrition [6,9].

Congo red staining

The sections were hydrated, background stained with haematoxylin and incubated in 50 ml of 80% ethanol saturated with NaCl and 0.5 ml 1% NaOH for 20 min and then incubated again for 20 min in 50 ml of 80% ethanol saturated with NaCl and Congo red and 0.5 ml 1% NaOH. Amyloid deposits were then visualized in polarized light.

Microwave antigen retrieval

The sections were treated as described in detail elsewhere [16]. Briefly, they were hydrated and immersed in 0.01 M citrate buffer (pH 6) in a plastic Coplin jar, which was placed in a microwave oven for 15 min at maximum power (650 W). The slides were allowed to cool to room temperature (20 °C) for 20 min, rinsed in TRIS buffer (pH 7.6) and then immunostained.

Immunohistochemistry

After the microwave antigen retrieval the sections were immunostained by the avidin–biotin complex (ABC) method (Dako, Glostrup, Denmark), as described previously in detail [10]. Briefly, specimens were immersed in 0.3% hydrogen peroxide in TRIS buffer (pH 7.6) for 10 min to inactivate endogenous peroxidase. They were then treated with 1% bovine serum albumin for 10 min to occupy the non-specific binding sites. The sections were incubated overnight with c-Kit (dilution 1:200, code no sc-168G, Santa Cruz Biotechnology, Santa Cruz, CA), TMEM16A (dilution 1:100, code no AP15524PU-M, Acris, Herford, Germany), protein gene product (PGP) 9.5 (dilution 1:600, code no M13C4, Ultra Clone, UK) and TTR (dilution 1:200, code no A0002, Dako, Glostrup, Denmark) antibodies at room temperature. Incubation with the secondary antibody, biotinylated rabbit anti-goat (for c-Kit) and rabbit anti-mouse IgG (for TMEM16A, PGP 9.5 and TTR) diluted 1:200, was carried out for 30 min at room temperature (20 °C). The specimens were then incubated with ABC (dilution 1:50 for PGP 9.5 and 1:200 c-Kit) at room temperature for 30 min. Peroxidase was detected by immersing the sections in 50 ml TRIS-buffer containing 25 mg diaminobenzidine tetrahydrochloride (DAB) and 10 µl of 30% H_2O_2 followed by counterstaining in Mayer's haematoxylin. The primary antibody was omitted on sections serving as negative controls.

Double staining

Double staining was performed using immunostaining with the ABC-method for PGP 9.5, c-Kit, TMEM16A, and TTR followed by staining with alkaline Congo red.

Computerized image analysis

All analyses were carried out on coded slides by one examiner (IA) who had no access to the code. Quantification was performed with the Quantimet 500 MC image processing and analysis system (Leica, Cambridge, UK) linked to an Olympus microscope, type BX50. The software was QWIN, a windows-based image analysis program, and QUIPS, an interactive programming system, both from Leica. Quantification was performed using a $\times 20$ objective (20X/0.5, UPlanFI, Olympus). At this magnification, one pixel of the image corresponded to 0.26 µm, and each field in the monitor represented a tissue area of 0.04 mm^2 .

To quantify the relative volume densities of TTR, nerves and ICC in the longitudinal and circular muscle layers, the classical stereological point-counting method as adapted for computerized image analysis was used [17–20]. The method is based on a mathematic model where the relative volume density of a structure (A) that lies within another structure (B) is calculated. Both structures occupy a certain volume and by numbering points covering the different structures a ratio, the relative volume density, between points covering structures A and B can be calculated.

Briefly, an automated standard sequence analysis operation was applied, in which a regular 400-point lattice was superimposed on the frame containing the tissue. Points covering tissue and points covering the TTR/nerves/ICC were

pointed out with the computer mouse by the examiner; by clicking on the mouse a series of blue highlighted points appeared. The ratio of points lying on TTR/nerves/ICC versus those lying on tissue in each field was tabulated. The sum of all fields in the specimen was computed and automatically analyzed with the QUIPS software. Twenty fields from the circular and longitudinal muscle layers, respectively, were randomly chosen from each individual. The ICC surrounding the myenteric plexa were not included in the analysis.

Statistical analysis

Statistical analysis was performed by non-parametrical methods since a normal distribution could not be guaranteed. Differences between groups were tested by the Mann–Whitney *U*-test and the Kruskal–Wallis test and correlations were tested by Spearman's rank order correlation. Data shown are medians (range). *p* values below 0.05 were regarded as statistically significant. PASW Statistics 18 for Macintosh was used for the calculations. Power calculations were retrospective and JavaStat [21] was used for the online calculations.

Ethics

The study was approved by a Japanese ethical committee, reference number: Kumamoto University No. 17-86.

Results

Patients

The patients' median age was 43 (36–63) years. The median duration of disease at the time of death and investigation was 11 (8–12) years and the median duration of the GI symptoms was 9 (6–11) years. All patients had suffered from diarrhoea and four (36 %) also from periods of constipation. Two (18%) of the patients had suffered from nausea. Patients' details are outlined in Table 1. The median age of the controls was 62 (24–85) years, which was significantly higher than for the patients ($z = 2.54$, $p = 0.010$). No data on GI symptoms were recorded for the control cases. Clinical data of the controls are presented in Table 2.

Nutritional status

mBMI data are presented in Tables 1 and 2. Median mBMI of the patients was 579 (430–806) and six patients (55%) had an

mBMI below 600 (severe malnutrition). Patients with diarrhoea as their only GI symptom had a lower mBMI than those with diarrhoea and nausea or alternating diarrhoea and constipation, but there was no significant difference in mBMI between the groups ($\chi^2 = 0.52$, $p = 0.77$).

Median mBMI of the controls was 555 (331–657) and eight (80%) of the controls had an mBMI below 600. There was no significant difference in mBMI between patients and controls ($z = 0.78$, $p = 0.47$).

Gastric ICC and nervous tissue

Figures 1, 2 and 3 show the results of the immunohistochemical procedures for c-Kit-immunoreactive (IR) ICC, TMEM16A-IR ICC and PGP 9.5-IR nervous tissue, respectively. There were strong correlations between the relative volume densities of c-Kit- and TMEM16A-IR ICC in both the circular and longitudinal muscular layers ($r^2 = 0.98$, $p < 0.001$, for both).

The relative volume densities of c-Kit-IR and TMEM16A-IR ICC were significantly lower in patients compared to controls. Median density of c-Kit-IR ICC was 0.00 versus 2.58 ($z = -2.98$, $p = 0.004$) in the circular muscle layers and 0.00 versus 1.84 ($z = -2.98$, $p = 0.004$) in the longitudinal muscle layers, for patients and controls, respectively (Figure 4A). Median density of TMEM16A-IR ICC was 0.00 versus 2.84 ($z = -2.76$, $p = 0.008$) in the circular muscle layers and 0.00 versus 1.46 ($z = -2.68$, $p = 0.010$) in the longitudinal muscle layers, for patients and controls, respectively.

There was no significant difference between the densities of PGP 9.5-IR nervous tissue in the circular muscle layer of patients and controls (median density 2.97 versus 6.76, $z = -1.41$, $p = 0.173$). In the longitudinal muscle layer, the densities of PGP 9.5-IR tissue tended to be lower in patients than in controls (median density 1.42 versus 2.47, $z = -1.66$, $p = 0.099$), however, the difference did not reach statistical significance (Figure 4B). No significant difference in the number of enteric neurons in myenteric ganglia was observed between patients and controls (median count 19.00 versus 14.50, $z = 0.85$, $p = 0.43$).

Gastric amyloid deposits

Amyloid deposits were detected in all sections from the patients, predominantly in the walls of the blood vessels. A massive amyloid infiltration was observed in the

Table 1. Clinical data of the patients.

Patient	Gender	Age (years)	GI symptom(s)	mBMI
1	F	43	Diarrhoea	484
2	M	61	Diarrhoea	430
3	M	36	Diarrhoea and nausea	626
4	F	41	Diarrhoea	543
5	M	38	Alternating diarrhoea/constipation	717
6	F	57	Diarrhoea	481
7	F	43	Alternating diarrhoea/constipation	611
8	M	52	Alternating diarrhoea/constipation	680
9	M	42	Alternating diarrhoea/constipation	806
10	F	63	Diarrhoea	525
11	F	48	Diarrhoea and nausea	579

F = female. M = male. GI = gastrointestinal. mBMI = modified body mass index, BMI (kg/m^2) \times serum albumin (g/L).

Table 2. Clinical data of the controls.

Control	Gender	Age (years)	Cause of death	mBMI
1	M	63	T-cell leukaemia	542
2	F	85	AMI	537
3	F	58	AMI	581
4	M	61	Lung cancer	421
5	M	75	Colon cancer	567
6	M	59	Colon cancer	331
7	M	77	Colon cancer	657
8	M	59	Colon cancer	527
9	M	66	Lymphoma	655
10	F	24	Colon cancer	568

AMI = acute myocardial infarction.

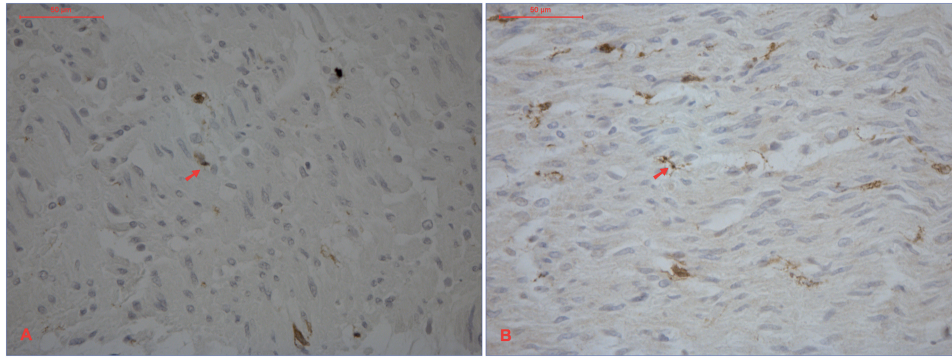


Figure 1. Immunohistochemical analyses of gastric antrum wall autopsy specimens visualizing c-Kit-IR ICC (dark brown) in (A) a patient with hereditary TTR amyloidosis and (B) a non-amyloidosis control. A $\times 40$ objective ($40\times/0.70$, PI Fluotar, Leica) was used for the analyses. IR = immunoreactive. ICC = interstitial cells of Cajal. TTR = transthyretin.

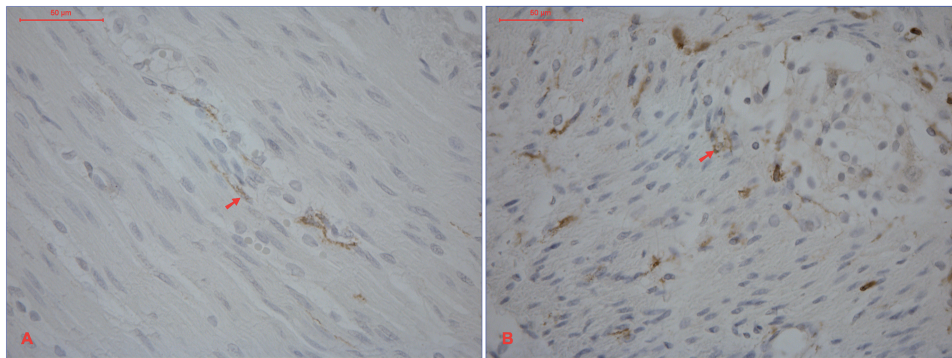


Figure 2. Immunohistochemical analyses of gastric antrum wall autopsy specimens visualizing TMEM16A-IR ICC (dark brown) in (A) a patient with hereditary TTR amyloidosis and (B) A non-amyloidosis control. A $\times 40$ objective ($40\times/0.70$, PI Fluotar, Leica) was used for the analyses.

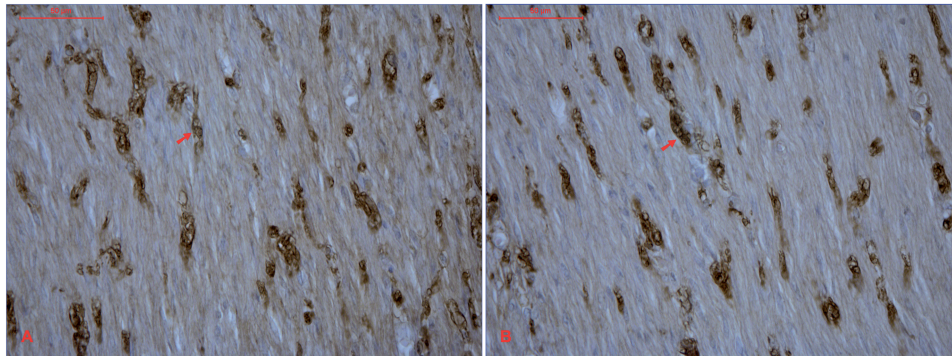


Figure 3. Immunohistochemical analyses of gastric antrum wall autopsy specimens visualizing PGP 9.5-IR nervous tissue (dark brown) in (A) a patient with hereditary TTR amyloidosis and (B) A non-amyloidosis control. A $\times 40$ objective ($40\times/0.70$, PI Fluotar, Leica) was used for the analyses. PGP 9.5 = protein gene product 9.5.

muscularis mucosae. There were also amyloid deposits in the muscularis externa and the submucosae in all sections from the patients.

The median relative volume density of amyloid deposits was 4.10 (1.16–38.23). There were no significant correlations between the densities of gastric amyloid deposits and c-Kit-IR ICC in the circular or longitudinal muscle layers ($r^2 = -0.56$, $p = 0.073$ and $r^2 = -0.58$, $p = 0.059$, respectively).

Also were there no significant correlations between the densities of gastric amyloid deposits and PGP 9.5-IR nervous tissue in the circular or the longitudinal muscle layers ($r^2 = 0.11$, $p = 0.75$ and $r^2 = 0.073$, $p = 0.83$, respectively).

Double staining showed that the amyloid deposits were located between or around, not within, the c-Kit-, TMEM16A- and PGP 9.5-IR areas. Also were there no amyloid deposits inside the myenteric plexa.

Gastric TTR

TTR immunohistochemistry was performed in all sections from the patients and the median relative volume density of TTR-IR tissue was 4.90 (1.96–40.10). No TTR-IR tissue was located outside the amyloid deposits and there was a strong correlation between the densities of amyloid deposits and TTR-IR tissue ($r^2 = 0.91$, $p < 0.001$).

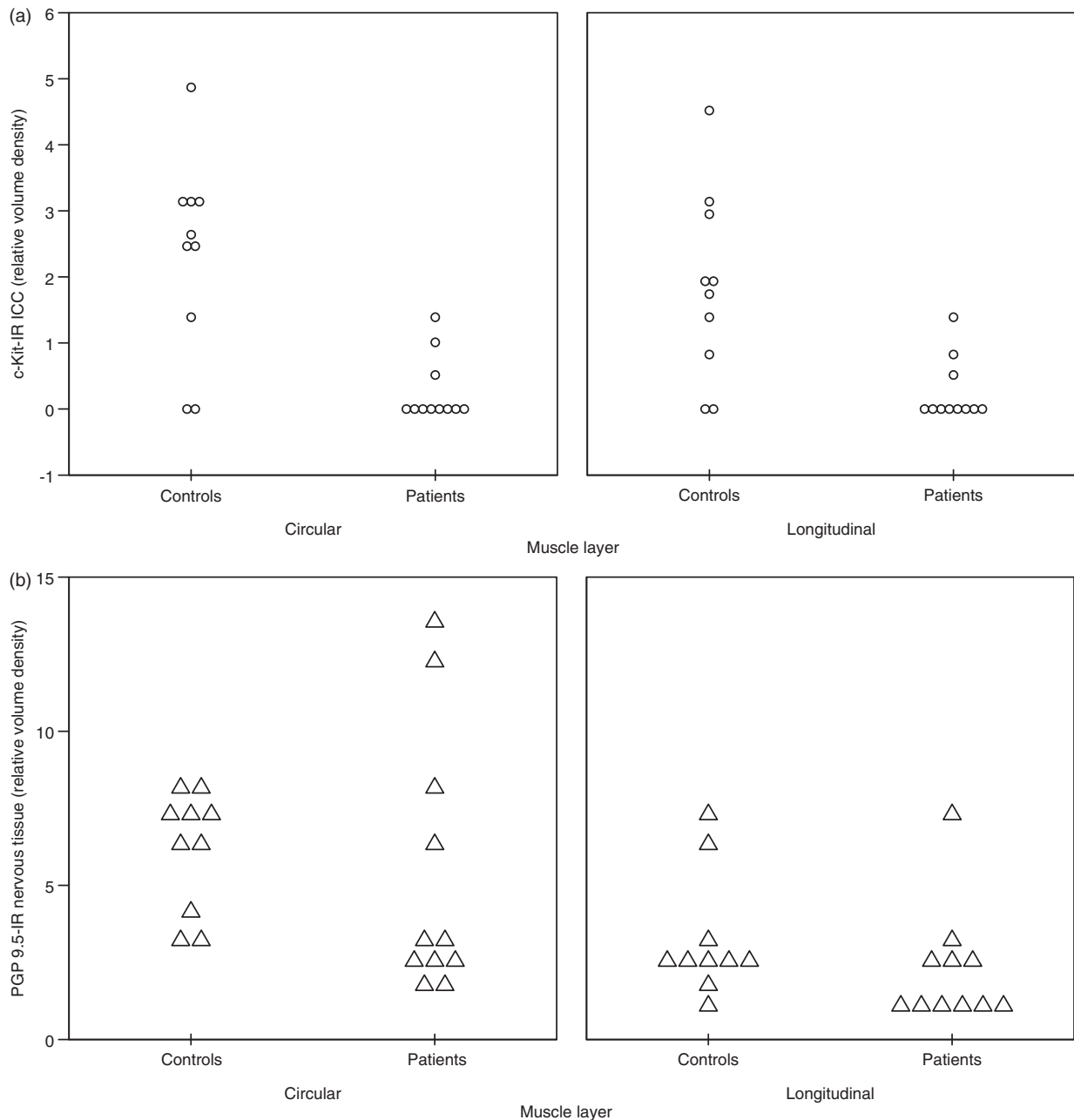


Figure 4. The relative volume densities of gastric c-Kit-IR ICC and PGP 9.5-IR nervous tissue in patients with hereditary TTR amyloidosis and non-amyloidosis controls were quantified with immunohistochemistry and computerized image analysis. (A) There were significant differences in c-Kit-IR ICC in both the circular and longitudinal muscle layers ($z = -2.98$, $p = 0.004$, for both). (B) No significant differences in PGP 9.5-IR nervous tissue were found in the circular or longitudinal muscle layers ($z = -1.41$, $p = 0.173$ and $z = -1.66$, $p = 0.099$, respectively).

Nutritional status and gastric ICC

We found no significant correlations between the patients' mBMI and their relative volume densities of c-Kit-IR ICC in the circular or longitudinal muscle layers ($r^2 = -0.32$, $p = 0.33$ and $r^2 = -0.44$, $p = 0.18$, respectively). Also were there no significant correlations between the controls' mBMI and their densities of c-Kit-IR ICC in the circular or longitudinal muscle layers ($r^2 = -0.29$, $p = 0.42$ and $r^2 = -0.16$, $p = 0.65$, respectively).

Age, gastric ICC and nervous tissue

There were no significant correlations between the age at death and the densities of c-Kit-IR ICC or PGP 9.5-IR

Table 3. Correlations between age at death and the relative volume densities of gastric c-Kit-IR interstitial cells of Cajal (ICC) and PGP 9.5-IR nervous tissue, respectively.

Age	ICC circ	ICC long	Nerves circ	Nerves long
Patients	$r^2 = 0.01$ $p = 0.97$	$r^2 = 0.24$ $p = 0.47$	$r^2 = -0.47$ $p = 0.15$	$r^2 = -0.48$ $p = 0.14$
Controls	$r^2 = 0.28$ $p = 0.43$	$r^2 = 0.40$ $p = 0.26$	$r^2 = 0.12$ $p = 0.74$	$r^2 = -0.13$ $p = 0.71$

IR = immunoreactive. Circ = circular muscle layer. Long = longitudinal muscle layer.

Table 4. Gender related differences in the relative volume densities of gastric c-Kit-IR interstitial cells of Cajal (ICC) and PGP 9.5-IR nervous tissue.

	ICC circ	ICC long	Nerves circ	Nerves long
Patients				
Females	0.00 (0.00–0.57)	0.00 (0.00–1.33)	3.14 (1.50–8.19)	1.20 (0.76–2.23)*
Males	0.00 (0.00–1.45)	0.00 (0.00–0.82)	2.61 (2.25–13.55)	2.72 (1.06–7.17)*
Controls				
Females	1.41 (0.00–2.51)	1.74 (0.00–1.94)	6.98 (3.24–8.37)	2.44 (2.35–2.86)
Males	3.08 (0.00–4.87)	1.93 (0.00–4.52)	6.54 (3.30–7.95)	2.50 (1.22–7.62)

Data shown are medians (range).

*Statistically significant difference.

nervous tissue in patients or controls. Details are outlined in Table 3.

Gender-related differences

We found no significant gender related differences in the densities of c-Kit-IR ICC in the circular or longitudinal muscle layers of patients ($z = 1.05$, $p = 0.429$ and $z = 0.58$, $p = 0.66$, respectively) or controls ($z = 1.60$, $p = 0.117$ and $z = 0.69$, $p = 0.52$, respectively).

For PGP 9.5-IR nervous tissue there was a significant gender-related difference in the longitudinal ($z = 2.19$, $p = 0.030$), but not in the circular muscle layer ($z = 0.55$, $p = 0.66$) of the patients. No significant differences were observed in the circular ($z = -0.11$, $p = 1.00$) or longitudinal muscle layers ($z = 0.11$, $p = 1.00$) of the controls. Details are outlined in Table 4.

Power

The calculated power to detect a difference in c-Kit-IR ICC between patients and controls was 82%.

Discussion

Gastrointestinal symptoms are common in hereditary TTR amyloidosis and are important for morbidity and mortality, both before and after liver transplantation [6,9]. All patients included in the present study suffered from GI complications and 55% showed signs of severe malnutrition. A majority (80%) of the controls also had mBMI values consistent with severe malnutrition.

To the best of our knowledge, this is the first study showing a depletion of gastric ICC in patients with TTR amyloidosis and the loss of ICC was verified with two different immunohistochemical procedures. We believe that this is an important factor for the GI disturbances in these patients and, since the controls were randomly selected and their cause of death was shifting, we find it unlikely that factors other than the TTR amyloidosis could explain the difference in ICC between patients and controls. Additionally, there was no significant difference in nutritional status between patients and controls and consequently, the difference in ICC was not caused by a poorer nutritional status of the patients.

The material is unique given the short time span between the time of death and the autopsies, which all were carried out by a pathologist on call. For this reason we had no possibility to select an age, gender and mBMI matched control material.

The fact that the median age was significantly higher in the control group may have influenced the densities of ICC and

nervous tissue in the controls; however, there were no significant correlations between age and the densities of ICC or nervous tissue in our material. There was an unequal gender distribution between the studied groups, but we found no evidence of any gender-related differences in the densities of ICC. For patients, there was a significant gender related difference in the densities of nervous tissue in one of the muscle layers, females showing a lower median density than males. This was not the case for the control group, which may be due to the larger proportion of males in this group. However, we do not believe that this is of any clinical significance.

The mechanisms behind the depletion of ICC are not clear. In analogy to previous data [20,22], we found no significant destruction of the enteric nervous system and consequently, an enteric neuropathy does not seem to be a major factor for the loss of ICC or for the GI symptoms in general. Further, there was no evidence of amyloid deposits within the c-Kit-IR or TMEM16A-IR areas of the patients, yet there was a trend to a negative correlation between the densities of amyloid and ICC, indicating that the amyloid deposits elicit indirect (i.e. toxic) rather than structural effects on the ICC. This also seems to be the case for the neurodegeneration in TTR amyloidosis [4]. The fact that the amyloid deposits were mostly found in the blood vessel walls, which is consistent with previous findings [22], might suggest that vascular changes contribute to the loss of ICC and to the GI complications in these patients.

Amyloid deposits in the autonomic and enteric nervous systems and changes in the neuroendocrine cell content of the GI tract may also be part of the underlying mechanisms [10–14]. However, as mentioned above, some studies show that the enteric nervous system is not affected in ATTR V30M patients and there was only a weak correlation between the autonomic function and the gastric emptying rates in another of our studies [23]. Moreover, the GI function is not improved after liver transplantation [24,25], although a normalization of the endocrine cell count can be observed [26]. An autonomic dysfunction is indeed important for some of the complications in patients with hereditary TTR amyloidosis, but it remains unclear to what extent the autonomic and enteric neuropathies affect their gastrointestinal function.

The preservation of ICC in the GI tract is dependent on a complex interaction of promoting and demoting factors involving stimulation of precursor cells, cell death and transdifferentiation of ICC into other cell types [27]. An imbalance between these promoting and demoting factors may contribute to the depletion of ICC.

As diabetes mellitus and hereditary TTR amyloidosis both cause autonomic and peripheral neuropathies and give rise to similar GI complications [7,28], it is tempting to believe that they share a common pathophysiology. Diabetics show a deficiency of gastric [29] as well as colonic ICC [30], which is believed to be one of the mechanisms behind their GI complications [31]. A depletion of smooth muscle cell-produced stem cell factor, due to relative insulinopenia and IGF-1 deficiency, and an increased oxidative stress have been shown to contribute to the loss of ICC in diabetes mellitus [32].

Patients with hereditary TTR amyloidosis show alterations in glucose metabolism [33] and decreased levels of growth hormone [34], a stimulator of IGF-1 production, which might suggest that hormonal changes affect the number of ICC also in TTR amyloidosis. Furthermore, there is evidence of amyloid toxicity and an increased oxidative stress in the amyloid deposits of patients with hereditary TTR amyloidosis [4,35,36], possibly mediated by AGE and RAGE [3], which accordingly may be another factor leading to a depletion of ICC in these patients.

At present there are few treatment options for the GI symptoms in patients with hereditary TTR amyloidosis and diabetes mellitus. Although a liver transplantation reduces the free radical activity in the amyloid deposits of patients with TTR amyloidosis [37], no improvement of the GI symptoms has been noted after liver transplantation [24,25]. Treatment aimed to counteract oxidative stress has been shown to be promising in patients with diabetes [38–40], but unfortunately there was no decrease in lipid peroxidation in amyloid deposits after 6 months of scavenger treatment with vitamin C and E and acetylcysteine in patients with TTR amyloidosis [41]. Bacterial overgrowth can be treated with antibiotics and prokinetic drugs can be used in patients with a delayed gastric emptying, however, mostly with only temporary effects on the symptoms. Therefore, there is a need for alternative approaches.

Limitations

As full-thickness gastric wall samples were required for the analyses of myenteric ICC, and as such samples are not available for living patients, all sections analyzed in the study were post-mortem samples, and thus a certain degree of post-mortem degradation was inevitable. However, all tissue samples except one were collected within 5 hours post mortem to minimize the tissue degradation. Further, the post-mortem degradation should be equivalent in the samples from patients and controls since the collecting procedure was the same in both groups.

The study was based on a small number of patients, which may have affected its outcome. Nevertheless, the calculated statistical power for the difference in c-Kit-IR ICC between patients and controls was 82%.

We chose to investigate the densities of gastric ICC and gastric nerves and one may argue that it would be better to use small intestinal or colonic tissues since most patients in the study suffered from lower GI symptoms. However, the depletion of ICC in patients with diabetes mellitus is reported to be similar throughout the GI tract [29,30] and the GI

symptoms has been shown to be poor predictors of the actual GI function in patients with TTR amyloidosis [23].

Both age and morbidity may have negatively affected the densities of ICC in the control group [42,43], which also indicates the absence of ICC in some control cases. No data on the relative volume densities of gastric PGP 9.5-IR nervous tissue or c-Kit- and TMEM16A-IR ICC of healthy controls were available to us at the time of the study.

Conclusions

Patients with hereditary TTR amyloidosis display a marked loss of gastric ICC compared to non-amyloidosis controls, but no evident depletion of intramural or myenteric gastric nerves. The loss of ICC, possibly mediated by amyloid toxicity and vascular changes, may well be an important factor for the GI disturbances in these patients.

Acknowledgements

Special thanks to Professor Ole B. Suhr, who contributed with his extensive knowledge in the field.

Declaration of interest

The study was supported by grants from the patients' organizations FAMY/AMYL in the counties of Västerbotten and Norrbotten, Umeå University, Spearhead grants from Västerbotten's county, ALF-grants from Norrlands University Hospital and a grant from the 6th research framework of EU, the EURAMY project.

The authors report no conflicts of interest. The authors alone are responsible for the content and writing of this article.

References

1. Olsson M, Hellman U, Planté-Bordeneuve V, Jonasson J, Lång K, Suhr OB. Mitochondrial haplogroup is associated with the phenotype of familial amyloidosis with polyneuropathy in Swedish and French patients. *Clin Genet* 2009;75:163–8.
2. Saraiva MJ. Transthyretin amyloidosis: a tale of weak interactions. *FEBS Lett* 2001;498:201–3.
3. Matsunaga N, Anan I, Forsgren S, Nagai R, Rosenberg P, Horiuchi S, Ando Y, et al. Advanced glycation end products (AGE) and the receptor for AGE are present in gastrointestinal tract of familial amyloidotic polyneuropathy patients but do not induce NF-kappaB activation. *Acta Neuropathol* 2002;104:441–7.
4. Sousa MM, Saraiva MJ. Neurodegeneration in familial amyloid polyneuropathy: from pathology to molecular signaling. *Prog Neurobiol* 2003;71:385–400.
5. Andersson R. Familial amyloidosis with polyneuropathy. A clinical study based on patients living in northern Sweden. *Acta Med Scand Suppl* 1976;590:1–64.
6. Suhr O, Danielsson A, Holmgren G, Steen L. Malnutrition and gastrointestinal dysfunction as prognostic factors for survival in familial amyloidotic polyneuropathy. *J Intern Med* 1994;235:479–85.
7. Suhr OB, Svendsen IH, Andersson R, Danielsson A, Holmgren G, Ranlov PJ. Hereditary transthyretin amyloidosis from a Scandinavian perspective. *J Intern Med* 2003;254:225–35.
8. Tashima K, Suhr OB, Ando Y, Holmgren G, Yamashita T, Obayashi K, Terazaki H, et al. Gastrointestinal dysfunction in familial amyloidotic polyneuropathy (ATTR Val30Met) – comparison of Swedish and Japanese patients. *Amyloid* 1999;6:124–9.

9. Suhr O, Danielsson A, Rydh A, Nyhlin N, Hietala SO, Steen L. Impact of gastrointestinal dysfunction on survival after liver transplantation for familial amyloidotic polyneuropathy. *Dig Dis Sci* 1996;41:1909–14.
10. Anan I, El-Salhy M, Ando Y, Nyhlin N, Terazaki H, Sakashita N, Suhr O. Colonic endocrine cells in patients with familial amyloidotic polyneuropathy. *J Intern Med* 1999;245:469–73.
11. el-Salhy M, Suhr O, Stenling R, Wilander E, Grimelius L. Impact of familial amyloid associated polyneuropathy on duodenal endocrine cells. *Gut*. 1994;35:1413–8.
12. Nyhlin N, Anan I, el-Salhy M, Ando Y, Suhr OB. Endocrine cells in the upper gastrointestinal tract in relation to gastrointestinal dysfunction in patients with familial amyloidotic polyneuropathy. *Amyloid* 1999;6:192–8.
13. Yoshimatsu S, Ando Y, Terazaki H, Sakashita N, Tada S, Yamashita T, Suga M, et al. Endoscopic and pathological manifestations of the gastrointestinal tract in familial amyloidotic polyneuropathy type I (Met30). *J Intern Med* 1998;243:65–72.
14. Ikeda S, Yanagisawa N, Hongo M, Ito N. Vagus nerve and celiac ganglion lesions in generalized amyloidosis. A correlative study of familial amyloid polyneuropathy and AL-amyloidosis. *J Neurol Sci* 1987;79:129–39.
15. Mostafa R-M, Moustafa YM, Hamdy H. Interstitial cells of Cajal, the Maestro in health and disease. *World J Gastroenterol* 2010;16:3239–48.
16. Nyhlin N, el-Salhy M, Sandström O, Suhr O. Evaluation of immunohistochemical staining of human duodenal endocrine cells after microwave antigen retrieval. *Histochem J* 1997;29:177–81.
17. Weibel E, Elias H, eds. Introduction to stereologic principles. In: *Quantitative methods in morphology*. Berlin: Springer; 1967:89–98.
18. Weibel ER, Stäubli W, Gnägi HR, Hess FA. Correlated morphometric and biochemical studies on the liver cell. I. Morphometric model, stereologic methods, and normal morphometric data for rat liver. *J Cell Biol* 1969;42:68–91.
19. el-Salhy M, Sandström O, Näsström E, Mustajbasic M, Zachrisson S. Application of computer image analysis in endocrine cell quantification. *Histochem J* 1997;29:249–56.
20. Anan I, El-Salhy M, Ando Y, Forsgren S, Nyhlin N, Terazaki H, Sakashita N, et al. Colonic enteric nervous system in patients with familial amyloidotic neuropathy. *Acta Neuropathol* 1999;98:48–54.
21. Pezzullo JC. JavaStat – retrospective power calculations [Internet]. 2012. Available from: <http://statpages.org/postpowr.html> [last accessed 2013 Feb 5].
22. Anan I, El-Salhy M, Ando Y, Terazaki H, Suhr OB. Comparison of amyloid deposits and infiltration of enteric nervous system in the upper with those in the lower gastrointestinal tract in patients with familial amyloidotic polyneuropathy. *Acta Neuropathol* 2001;102:227–32.
23. Wixner J, Karling P, Rydh A, Hörnsten R, Wiklund U, Anan I, Suhr OB. Gastric emptying in hereditary transthyretin amyloidosis: the impact of autonomic neuropathy. *Neurogastroenterol Motil* 2012; 24:1111–e568.
24. Lång K, Wikström L, Danielsson A, Tashima K, Suhr OB. Outcome of gastrointestinal complications after liver transplantation for familial amyloidotic polyneuropathy. *Scand J Gastroenterol* 2000;35:985–9.
25. Suhr OB, Anan I, Ahlström KR, Rydh A. Gastric emptying before and after liver transplantation for familial amyloidotic polyneuropathy, Portuguese type (Val30Met). *Amyloid* 2003;10:121–6.
26. Anan I, El-Salhy M, Nyhlin N, Suhr OB. Liver transplantation restores endocrine cells in patients with familial amyloidotic polyneuropathy. *Transplantation* 2000;70:794–9.
27. Farrugia G. Interstitial cells of Cajal in health and disease. *Neurogastroenterol Motil* 2008;20:54–63.
28. Gatopoulou A, Papanas N, Maltezos E. Diabetic gastrointestinal autonomic neuropathy: Current status and new achievements for everyday clinical practice. *Eur J Intern Med* 2012;23:499–505.
29. Iwasaki H, Kajimura M, Osawa S, Kanaoka S, Furuta T, Ikuma M, Hishida A. A deficiency of gastric interstitial cells of Cajal accompanied by decreased expression of neuronal nitric oxide synthase and substance P in patients with type 2 diabetes mellitus. *J Gastroenterol* 2006;41:1076–87.
30. Nakahara M, Isozaki K, Hirota S, Vanderwinden J-M, Takakura R, Kinoshita K, Miyagawa J-I, et al. Deficiency of KIT-positive cells in the colon of patients with diabetes mellitus. *J Gastroenterol Hepatol* 2002;17:666–70.
31. Ördög T. Interstitial cells of Cajal in diabetic gastroenteropathy. *Neurogastroenterol Motil* 2008;20:8–18.
32. Kashyap P, Farrugia G. Diabetic gastroparesis: what we have learned and had to unlearn in the past 5 years. *Gut* 2010;59:1716–26.
33. Ando Y, Yi S, Nakagawa T, Ikegawa S, Hirota M, Miyazaki A, Araki S. Disturbed metabolism of glucose and related hormones in familial amyloidotic polyneuropathy: hypersensitivities of the autonomic nervous system and therapeutic prevention. *J Auton Nerv Syst* 1991;35:63–70.
34. Olofsson BO, Grankvist K, Olsson T, Boman K, Forsberg K, Lafvas I, Lithner F. Assessment of hypothalamic-pituitary function in patients with familial amyloidotic polyneuropathy. *J Intern Med* 1991;229:55–9.
35. Ando Y, Nyhlin N, Suhr O, Holmgren G, Uchida K, El Sahly M, Yamashita T, et al. Oxidative stress is found in amyloid deposits in systemic amyloidosis. *Biochem Biophys Res Commun* 1997;232:497–502.
36. Hou X, Aguilar M-I, Small DH. Transthyretin and familial amyloidotic polyneuropathy. Recent progress in understanding the molecular mechanism of neurodegeneration. *FEBS J* 2007;274:1637–50.
37. Nyhlin N, Anan I, El SM, Ando Y, Suhr OB. Reduction of free radical activity in amyloid deposits following liver transplantation for familial amyloidotic polyneuropathy. *J Intern Med* 2002;251:136–41.
38. Choi KM, Kashyap PC, Dutta N, Stoltz GJ, Ördög T, Shea Donohue T, Bauer AJ, et al. CD206-positive M2 macrophages that express heme oxygenase-1 protect against diabetic gastroparesis in mice. *Gastroenterology* 2010;138:2399–2409.
39. Bharucha AE, Kulkarni A, Choi KM, Camilleri M, Lempke M, Brunn GJ, Gibbons SJ, et al. First-in-human study demonstrating pharmacological activation of heme oxygenase-1 in humans. *Clin Pharmacol Ther* 2010;87:187–90.
40. Kashyap PC, Choi KM, Dutta N, Linden DR, Szurszewski JH, Gibbons SJ, Farrugia G. Carbon monoxide reverses diabetic gastroparesis in NOD mice. *Am J Physiol Gastrointest Liver Physiol* 2010;298:G1013–19.
41. Suhr OB, Lång K, Wikström L, Anan I, Ando Y, El-Salhy M, Holmgren G, et al. Scavenger treatment of free radical injury in familial amyloidotic polyneuropathy: a study on Swedish transplanted and non-transplanted patients. *Scand J Clin Lab Invest* 2001;61:11–8.
42. Gomez-Pinilla PJ, Gibbons SJ, Sarr MG, Kendrick ML, Robert Shen K, Cima RR, Dozois EJ, et al. Changes in interstitial cells of cajal with age in the human stomach and colon. *Neurogastroenterol Motil* 2011;23:36–44.
43. Donthireddy KR, Ailawadhi S, Nasser E, Schiff MD, Nwogu CE, Nava HR, Javle MM. Malignant gastroparesis: pathogenesis and management of an underrecognized disorder. *J Support Oncol* 2007;5:355–63.